Published in final edited form as:
Ann Neurol. 2011 September ; 70(3): 465–476. doi:10.1002/ana.22484.

White Matter Lesions Defined by Diffusion Tensor Imaging in Older Adults

Stephen A. Back, M.D., Ph.D.[1,2], **Christopher D. Kroenke, Ph.D.**[3,5], **Larry S. Sherman, Ph.D.**[4,6], **Gus Lawrence, B.S.**[1], **Xi Gong, M.D.**[1], **Erin N. Taber, B.S.**[5], **Joshua A. Sonnen, M.D., Ph.D.**[7], **Eric B. Larson, M.D.,M.P.H.**[8], and **Thomas J. Montine, M.D., Ph.D.**[2,7]

[1]Department of Pediatrics, Oregon Health & Science University, Portland, Oregon

[2]Department of Neurology, Oregon Health & Science University, Portland, Oregon

[3]Department of Behavioral Neuroscience, Oregon Health & Science University, Portland, Oregon

[4]Department of Cell and Developmental Biology, Oregon Health & Science University, Portland, Oregon

[5]Advanced Imaging Research Center, Oregon Health & Science University, Portland, Oregon

[6]Division of Neuroscience, Oregon National Primate Research Center, Beaverton, Oregon

[7]Department of Pathology, University of Washington, Seattle, Washington

[8]Group Health Research Institute, Seattle, Washington.

Abstract

Objective—The cellular and molecular mechanisms underlying MRI-defined white matter (WM) changes associated with age-related cognitive decline remain poorly defined. We tested the hypothesis that WM lesions in older adults, defined by diffusion tensor imaging (DTI), arise in the setting of vascular brain injury (VBI) and are characterized by increased free radical injury and aberrant oligodendrocyte lineage (OL) cell response to injury.

Methods—We undertook a multimodal analysis of prefrontal cortex (PFC) WM from twenty-five autopsies derived from a population-based cohort where VBI and Alzheimer's Disease (AD) frequently coincide. *Ex-vivo* high field strength DTI measurements of fractional anisotropy (FA), apparent diffusion coefficient (ADC), and axial ($D_{\parallel}$) and radial ($D_{\perp}$) diffusivity were measured at high magnetic field strength (11.7 T) and analyzed relative to quantitative *in vivo* biomarkers of free radical injury, an OL-specific marker Olig2, and histologic evaluation of hyaluronan (HA), an inhibitor of OL maturation.

Results—Coincident AD and VBI showed significant association with lower FA and a robust relationship between decreasing FA and increasing $D_{\perp}$. Free radical injury to docosahexaenoate and adrenate in PFC WM was significantly elevated in cases with VBI independent of AD, and were inversely correlated with FA. Similarly, increased density of Olig2-immunoreactive cells in PFC WM was significantly associated with VBI independent of AD and co-localized with regions enriched in HA.

Interpretation—DTI-defined PFC WM lesions in older individuals are characterized by free radical injury to myelin and neuro-axonal elements that coincides with pronounced expansion of the pool of OL cells in HA-rich regions.

Correspondence to: Thomas J. Montine, MD, PhD Department of Pathology Box 359791 University of Washington Seattle, WA 98104.

Keywords

white matter; vascular brain injury; Alzheimer's disease; diffusion tensor imaging; oxidative damage; oligodendroglia

Age-related cognitive decline classically has been associated with decreased synaptic density and neuron loss. However, growing evidence supports a central role for white matter (WM) changes in cognitive dysfunction associated with both normative and pathological aging. Indeed, sixty-five percent of cognitively normal individuals >75 years of age show WM abnormalities,[1,2] including diffuse changes as well as small infarcts,[3] and neuroimaging correlates of cognitive performance in elderly individuals have identified WM as a primary site of damage.[4-8] While the most common location of WM changes in the adult brain is the periventricular region, some neuroimaging studies of age-related WM changes have highlighted an apparent specific vulnerability of frontal WM fiber systems relative to other brain regions.[9,10] Correlation of regional WM hyperintensities with impairment in specific cognitive domains is an area of intense current investigation that is not in complete agreement; however, several studies have observed an association between age-related impairment in executive function or complex processing speed and anterior WM hyperintensities that is either focused on, or at least includes, frontal lobe WM.[8,11,12]

More recently, WM changes have been investigated using diffusion tensor imaging (DTI), an MRI technique that provides information about WM integrity through measurements of water diffusion and its directional dependence.[13,14] Several DTI studies, as well as related MRI measurements of transverse relaxation rates,[15] have observed age-associated WM changes that commonly involve prefrontal cortex (PFC), centrum semiovale, and anterior callosal regions, and which are associated with impaired cognitive function (reviewed in [16]; [17-22]). The disease mechanisms responsible for these WM changes remain elusive, and this has hampered the development of relevant animal models and therapeutic strategies. In fact, it is currently unclear if these DTI measures of WM changes result from demyelination, axonal loss, or other alterations in WM.[23]

One potential etiology for cerebral WM injury in the elderly is chronic hypoperfusion due to small vessel disease.[24,25] Indeed, a number of vascular changes that result in reduced cerebral blood flow, including hypoxia-induced capillary loss, reduced cerebrovascular angiogenesis, and tortuous arterioles, each may contribute to WM damage in older individuals.[26,27] However, how such potential hypoperfusion may damage WM in older adults is unclear. A mechanism for hypoperfusion-mediated WM damage in preterm infants has been the recent focus of both experimental models and observational studies using human tissue. This work has identified maturation-dependent vulnerability of oligodendrocyte lineage (OL) cells to injury initiated by ischemia and its associated free radical damage[28,29] that results in an initial expansion of the oligodendrocyte precursor pool and reactive astrogliosis.[30] Importantly, chronic WM injury triggers maturation arrest of OL cells that are especially vulnerable to recurrent ischemic injury,[31] and growing evidence suggests that this OL maturation arrest is linked to the accumulation of the glycosaminoglycan hyaluronan (HA) generated by reactive astrocytes and other cells in lesion microenvironments.[29,32,33] Interestingly, a previous study of animal models of both ischemia and Alzheimer's Disease (AD) demonstrated similarly expanded OL cells in adult animals,[34] raising the possibility that similar mechanisms may occur in older humans.

To determine whether a similar mechanism is potentially operative, and underlies DTI changes associated with aging in frontal WM of older adults, we undertook a multimodal analysis of WM change in human autopsy cases from a population-based cohort where

Vascular Brain Injury (VBI) and AD are prevalent. Specifically, we determined the relationships among AD, VBI, DTI-defined changes in WM, free radical injury, and pathological responses by cells in the OL lineage relative to HA accumulation.

Methods

Study Population and Tissue Collection

We collected twenty-five human right prefrontal cortex (PFC) WM samples from consecutive autopsies in the Adult Changes in Thought (ACT) study, an ongoing prospective longitudinal population-based study of brain aging and incident dementia in men and women[35,36] that had: (i) post-mortem interval < 8 hr, (ii) last clinical evaluation < 24 month before death, and (iii) no grossly identified lesion in the frontal lobes. Only three subjects had a MRI during life as part of their clinical care. PFC WM was collected using the rostral and caudal tips of the olfactory bulbs as external landmarks. Medial right frontal cortex that contained the orbito-frontal cortical gray matter (GM) was retained for purposes of orientation for MRI. The immediately rostral 2-3 mm of WM was flash frozen in liquid nitrogen and stored at -80°C for quantification of isoprostanoids. The caudal block (~1cm×1cm×2cm) was immersion fixed in 4% paraformaldehyde (PFA) for 48 h and stored thereafter at 4°C in PBS with 0.01% sodium azide. For comparison with human samples, we collected flash frozen PFC WM from rhesus macaques as described previously.[37]

Neuropathologic Evaluation

Extensive neuropathologic examination of brain was performed according to previously published methods.[38] Microscopic examination for diseases that commonly contribute to cognitive impairment or dementia was performed using our established protocols.[38] These included evaluation of AD by NIA-Reagan Institute criteria, which employs Consortium to Establish a Registry for AD (CERAD) neuritic plaque (NP) score and Braak stage for neurofibrillary tangles (NFTs);[39] vascular-based injury (VBI) by cerebral microvascular infarct (CMI) number;[38,40] and Lewy body disease (LBD).[41]

Quantification of Free Radical Injury

We quantified F_2-Isoprostanes (IsoPs), F_4-Neuroprostanes (NeuroPs), and F_2-Adrenoprostanes (AdrenoPs) from the same flash frozen PFC WM using a stable isotope dilution assay with gas chromatography/mass spectrometry and selective ion monitoring (GC/MS/SIM). Tissue preparation for quantification of all three isoprostanoids has been described.[42] F_2-IsoPs derive from arachidonic acid (AA), which is evenly distributed in all cell types, and thus is an excellent marker to quantify free radical damage to all tissue components.[43,44] F_4-NeuroPs derive from docosahexaenoic acid (DHA) and provide highly specific data on free radical injury to neuronal membranes;[45] in WM these are largely axonal membranes. F_2-AdrenoPs derive from adrenic acid (AdA),[42] which in humans and other primates provide a specific marker of free radical damage to myelin.[42]

Diffusion Tensor Ex-vivo Magnetic Resonance Imaging

Tissue was immersed in PBS within a 2.5-cm diameter tube alongside a parietal tissue block from the same hemisphere, or PFC from the left hemisphere. A 3.5-cm diameter, 3.5-cm in length, single-turn solenoidal coil was utilized for radiofrequency transmission and reception. Experiments were performed using a 11.7 T magnet interfaced with a 9-cm inner diameter magnetic field gradient coil (Bruker, Rheinstetten, Germany). Procedures generally followed the previously published strategy that used DTI to characterize postmortem tissue from non-human primates.[46-48] A Stejskal-Tanner multi-slice spin-echo pulse sequence with parameters δ = 12 ms, Δ = 21 ms, and G = 11.6 G/cm (resulting in b = 2.5 ms/μm^2) was

used to perform DTI measurements. The *b*-value for this study was selected to provide an approximate match in diffusion sensitization to a typical *in vivo* measurement in which b = 1 ms/μm^2 (the water apparent diffusion coefficient is approximately 2.5-fold smaller in post-mortem tissue than *in vivo*.[49] Diffusion anisotropy measurements were made using a 25-direction, icosahedral sampling scheme[50] in combination with two measurements in which *b* = 0. Other pulse sequence settings were TR = 6.6 s, TE = 42 ms, NEX (the number of averaged transients) = 1, and image resolution was isotropic, with voxel dimensions of (0.5 mm)^3 and a 32 mm (phase-encode) by 64 mm (readout) by 30 mm (slice-select) field of view.

Standard procedures[50] were followed to determine eigenvalues (λ_1, λ_2, and λ_3, listed from smallest to largest) and corresponding eigenvectors of the diffusion tensor, as well as the signal amplitude in the absence of diffusion weighting, for each voxel from the set of 27 3D images. The apparent diffusion coefficient (ADC = ($\lambda_1 + \lambda_2 + \lambda_3$)/3), fractional anisotropy (FA, defined in [51]), axial diffusivity ($D_{\parallel} = \lambda_3$), and radial diffusivity ($D_{\perp} = (\lambda_1 + \lambda_2)/2$) were calculated from the eigenvalues for each voxel. The image consisting of signal amplitude in the absence of diffusion weighting exhibits contrast characteristic of a T_2-weighted image. Voxels for each tissue block were manually classified by an individual who was blinded to neuropathologic classification as either GM or WM using the derived T_2-weighted image, and standard functionalities of the ITK-snap program[52] (http://www.itksnap.org/pmwiki/pmwiki.php). Mean values for DTI-derived parameters within WM reported herein for a given case are computed as means over the set of voxels classified as WM.

Histochemical or Immunohistochemical Studies and Quantification of OL lineage cells

After MRI studies were completed, tissue blocks were serially sectioned free-floating (50 μm) in PBS with a Leica VTS-1000 vibrating microtome. Luxol fast blue (LFB) histochemistry for myelin and 2F11 (Dako, Carpinteria, CA) immunohistochemistry for neurofilament protein (an axonal marker) were performed on sections from each block. Scoring of LFB stain for myelin and 2F11 immunohistochemistry were performed as previously described.[61] To visualize total OL lineage cells, sections were first treated for antigen retrieval by incubation for 10 min at 95°C in 10 mM sodium citrate buffer, pH 6.0. Tissue was incubated with a rabbit polyclonal antiserum (1:10,000 in PBS with 0.1% triton X-100) raised against the nuclear transcription factor Olig2 (generous gift of Dr. John Alberta, Dana Farber Cancer Institute, Boston). The primary antiserum was visualized with a goat anti-rabbit biotinylated secondary antibody (1:200, 111-065-046; Jackson ImmunoResearch, WestGrove, PA) and a peroxidase-immunoperoxidase staining protocol with nickel silver enhancement (SK-4100; Vector Laboratories, Burlingame, CA). For double-labeling to visualize Olig2 and HA, sections were stained first for Olig2 as described above. Then, following the final wash after incubation with nickel silver enhancement reagent, sections were incubated with an HA-binding protein (HABP; 1:200; Seikagaku, Japan) as previously described.[29] HA was then visualized following incubation with avidin-peroxidase and a VIP substrate kit for peroxidase according to the manufacturer's instructions (SK-4600, Vector Laboratories). Within each section, high HA areas could be distinguished easily from low HA areas by staining intensity of the biotinylated-HABP (*e.g.*, Fig. 5). Counts of olig2+ cells were made only in areas that could be clearly delineated with intense HABP staining vs. weak staining. Mean cell densities were calculated and compared using a Student's t test.

The density of nuclei labeled with Olig2 was determined by an investigator blinded to pathological diagnosis from a minimum of 10 digitized bright-field images that were acquired in at least 3 near adjacent sections with a Leica DMRA upright microscope coupled to a Leica DFC 290 digital color camera. Digitized images were randomly but

systematically acquired by another investigator blinded to pathological diagnosis with a 40x objective within the boundaries of the cerebral WM or with a 20x objective within the boundaries of the cerebral cortex. Boundaries were defined with the aid of a methyl green counterstain.

Data and Analysis

All neuropathologic data were collected by certified neuropathologists without knowledge of clinical or laboratory results, all laboratory data were collected by scientists without knowledge of the clinical or neuropathologic diagnosis, and all laboratory groups generated their results without knowledge of results from each other's laboratories until all samples had been analyzed. After completing all data collection, results were analyzed as described using GraphPad Prism (San Diego, CA). The analytical strategy for comparison among the four pathologic groups (Figures 2G, 2H, 3B, 3C, and 4E) was two-way ANOVA for VBI, AD, and interaction between VBI and AD, followed by Bonferroni-corrected repeated paired comparisons; an identical approach was used for the four group data in Figure 4C. Comparison of two group data (Figure 5C and human *vs*. monkey isoprostanoid comparisons) used t test. Discontinuous rankings of morphological changes obtained by histochemical or immunohistochemical methods were correlated with MRI or isoprostanoid data using Spearman's ranked correlation. Continuous data were displayed by scatter plots, Pearson's correlation coefficient (r) calculated, or linear regression used to calculate the best-fit line (Figures 2F, 3A, and 4D). Alpha was set to 0.05.

RESULTS

Co-morbid AD and VBI is Common in Community-Derived Autopsy Brains

Our previous work with the ACT cohort has shown that AD and VBI are highly prevalent and commonly co-morbid, even in individuals who were not diagnosed with dementia during life.[38] Here, we studied a series of twenty-five consecutive ACT cases. Nine individuals were diagnosed with dementia, either probable AD (n=5) or mixed dementia (n=4) by DSM-IV criteria. Average ± SD last Cognitive Assessment Screening Instrument (CASI) score for subjects with dementia was 72 ± 12. The remaining sixteen Control individuals who did not meet these criteria for a diagnosis of dementia had last average CASI = 93 ± 3. In **Figure 1**, we have plotted a cumulative neuropathology score for each of the twenty-five cases and indicated (*) those who were diagnosed with dementia. We used the Braak stage for neurofibrillary tangles (NFTs, stages none to VI converted to 0 to 6) as a measure of the burden of AD and the total number of cerebral microinfarcts (CMIs) and cerebral lacunar infarcts as a measure of small vessel VBI burden, similar to how we have presented co-morbid diseases previously.[53] VBI was identified in 17 out of 25 cases. Territorial cerebral infarcts in regions other than the PFC were present in four individuals who also showed evidence of small vessel VBI. Consistent with our previous observations from hundreds of individuals in this cohort, those diagnosed with dementia within two years of death were over-represented among those with the greatest burden of VBI and AD. **Table 1** presents data on these twenty-five individuals now stratified by presence or absence of VBI and high (Braak stages IV to VI) vs. low (Braak stages none to III) AD. Neuritic plaque density was not used to categorize cases; however, the most common CERAD score in the Low AD group was “sparse” and in the High AD group was “frequent”. No case had cerebral cortical Lewy body disease. The four pathologic groups did not differ significantly by age, proportion that was women, post mortem interval, or brain weight.

Co-morbid AD and VBI was Significantly Associated with Reduced Fractional Anisotropy (FA)

We next employed DTI to define the relative contributions of AD and VBI burden to changes in FA or ADC in each case. The effects of low or high AD and VBI burden are illustrated by representative cases in **Figure 2**. First, we generated 3-D surface models of the fixed tissue (Fig. 2A). T_2-weighted images were used to classify image voxels as GM (used to aid in orientation) or WM (Fig. 2B). Fractional anisotropy (FA, Fig. 2C) and apparent diffusion coefficient (ADC, Fig. 2D) in individual slices are shown as parameter maps. Comparison to the sample from the Low AD/No VBI group demonstrates increased ADC and decreased FA in the case of severe damage from the High AD/VBI group.

FA and ADC were highly negatively correlated to each other ($r = -0.71$, $P<0.0001$) for the entire cohort. FA was more strongly correlated with $D_\perp$ ($r = -0.79$, $P < 0.0001$) than $D_\parallel$ ($r = -0.49$, $P < 0.05$). However, inspection of the scatter plot of $D_\perp$ and $D_\parallel$ vs. FA (Fig. 2E, asterisk) showed two cases with especially low FA that appeared to dominate the relationship between FA and ADC, particularly for $D_\parallel$. The two cases with very low PFC FA are marked in Figure 1. These were the two cases with highest VBI from among those with isocortical NFTs (Braak Stage V or VI), although there were other cases with similar levels of each pathologic change. We examined the other twenty-three PFC WM samples separately in an effort to unmask more subtle relationships among those with less heavily damaged PFC WM. $D_\parallel$ was not significantly associated with FA in this set of twenty-three cases. In contrast, $D_\perp$ continued to be negatively associated with FA in this large subset of cases with less extensively damaged WM (Fig. 2F). Analysis of mean FA or ADC for the groups described in Table 1 showed complementary changes in these DTI measures that were significant for FA in the High AD/VBI group but not for ADC (Figs. 2G,H). Although there are limitations to stratifying continuous MRI data into discrete pathologic categories, these results, nevertheless, suggest that DTI measures of PFC WM damage occur over a wide range and are most extensively altered by the combined presence of VBI and AD. Moreover, our results demonstrate a robust relationship between decreasing FA and increasing $D_\perp$ (usually interpreted as WM injury)[54] in post mortem PFC WM samples, and a more complex relationship between FA and $D_\parallel$ that may be especially sensitive to extreme WM injury.

WM Change Defined by DTI was Significantly Associated with Free Radical Injury

Since DTI changes were strongly related to VBI and one consequence of VBI is free radical injury, we tested the hypothesis that changes in DTI were correlated with quantitative *in vivo* measures of free radical injury. We determined isoprostanoid concentrations in flash frozen tissue blocks adjacent to those from which WM changes were measured by DTI. All samples were assayed twice. The average difference of replicates was 3.8%. F_2-IsoP ($r = -0.56$, $P < 0.01$), F_4-NeuroP ($r = -0.80$, $P < 0.0001$), and F_2-AdrenoP ($r = -0.84$, $P < 0.0001$) levels were negatively correlated with FA (Fig. 3A). ADC also was significantly correlated with F_4-NeuroP levels ($r = -0.55$, $P<0.01$) and F_2-AdrenoP levels ($r = -0.67$, $P<0.001$) across all twenty-five PFC WM samples. F_2-IsoP concentrations were not significantly correlated with ADC. Elimination of the two cases with lowest FA from these analyses did not alter the significance of the above relationships (not shown). There was not a statistically significant correlation between isoprostanoids and either $D_\perp$ or $D_\parallel$.

Isoprostanoid data were next stratified among the four pathologic groups. It is important to emphasize that there were no infarcts in the samples analyzed. Rather, classification of VBI was based on the presence of CMIs or lacunes in other cerebral regions. The average (±SEM) values for F_2-IsoPs and F_4-NeuroPs for the Low AD/No VBI and High AD/No VBI groups were similar to each other and to what we observed for F_2-IsoPs and F_4-NeuroPs in

normal cerebral WM from human neonates.[55] F_4-NeuroPs (Fig. 3B, $P < 0.01$) and F_2-AdrenoPs (Fig. 3C, $P < 0.05$) were significantly elevated in the VBI group, but not for Low vs. High AD or for interactions between VBI and AD; F_2-IsoPs were not significant among any of the groups. Corrected post-tests also showed that presence of VBI was associated with significantly increased F_4-NeuroPs and F_2-AdrenoPs in PFC WM regardless of the burden of AD pathologic changes in hippocampus or isocortical structures, although both indices of free radical injury were greatest in the combined High AD/VBI group, similar to DTI measures. These data indicate that free radical injury to PFC WM (i) was associated with VBI elsewhere in cerebrum, and (ii) was significantly linearly related to MRI-defined WM changes in adjacent tissue.

A potential limitation of biochemical measurements from human postmortem tissue are that changes of oxidative injury may occur during the agonal state or during the postmortem interval (PMI) between death and autopsy. While it is possible to correct statistically for effects of PMI, the much larger challenge is agonal state, which potentially can introduce artifacts and for which there is no adequate means of statistical correction. Therefore, we quantified these three isoprostanoids in PFC WM from 9 rhesus macaques aged 5-26 years (median=17) sacrificed for culling with no *post mortem* delay and no agonal state. The mean levels (± SEM) for macaque PFC WM were 3.1±0.1 for F_2-IsoPs, 16.4±2.2 for F_4-NeuroPs, and 16.5±1.9 ng/g for F_2-AdrenoPs. Hence, F_2-IsoPs in rhesus macaque PFC WM were significantly greater than Low AD/No VBI human PFC WM ($P<0.05$). Moreover, there was no difference between macaque and Low AD/no VBI human PFC WM F_4-NeuroPs or F_2-AdrenoPs ($P>0.40$ for both). These findings support that our observed differences in free radical damage to human PFC WM were not significantly confounded by conditions surrounding death or delay between death and autopsy.

Morphologic studies of myelin and axonal markers

Standard morphologic studies for myelin and the axonal marker neurofilament protein can be informative with respect to WM injury but are challenging to quantify and do not point to specific mechanisms of injury. With these limitations in mind, we performed LFB histochemistry to assess myelin and 2F11 immunohistochemistry to assess axons on each sample; each case was ranked by a blinded neuropathologist as not damaged (0), mildly (1), moderately (2), or severely (3) damaged, as judged by decreased staining intensity and structural disruption. Myelin damage rankings using LFB correlated with ADC ($P < 0.05$) but not FA. Axon damage ranking trended with F_4-NeuroPs ($P = 0.07$) but not with F_2-IsoPs, F_2-AdrenoPs, ADC, or FA.

OL Lineage Cells were Significantly Increased in Cases with VBI and AD

Studies in animal models have demonstrated that both focal ischemia and amyloid β deposition can cause an accumulation of cells that express the olig2 transcription factor.[34] In the adult brain, the olig2 transcription factor is typically expressed by OL cells and by NG2+ glial progenitor cells that differentiate into myelin-forming oligodendrocytes following demyelinating insults.[56-58]

We hypothesized a reactive OL response in WM following free radical injury. We determined in triplicate the density of OL cells with Olig2-immunoreactive nuclei (Olig2+) in PFC WM in each of the 25 cases described above (**Figure 4**). Whereas the isoprostanoid measurements were made from tissue adjacent to the block that underwent MRI, all immunohistochemical studies were performed on the same tissue block that was examined by MRI. The density of Olig2+ cells observed in the WM varied widely among cases from low (Fig. 4A) to high (Fig. 4B), with the latter indicative of a pronounced reaction. The density of Olig2+ cells typically was much greater in WM than the corresponding cortical

GM in our PFC samples ($P < 0.001$, Fig. 4C). Stratification by presence or absence of VBI showed increased Olig2+ cell density in WM ($P < 0.01$) but not in the overlying GM. Hence, nuclear Olig2 immunoreactivity identified a subset of cells that was greatly over-represented in WM relative to GM, and whose density in WM increased with VBI.

Among the twenty-three cases with less extreme WM injury, Olig2+ cell density had a negative linear relationship with FA ($P < 0.05$) and a positive linear relationship with ADC ($P < 0.05$). The latter was largely explained by $D_{\perp}$ and Olig2+ cell density ($P < 0.01$), but not $D_{\parallel}$ ($P > 0.15$), suggesting an association between WM injury and increased density of Olig2+ cells (Fig. 4D). Stratification of WM Olig2+ cell density into the four pathologic groups showed that increased Olig2+ cell density was associated with VBI ($P<0.05$) and not AD (Fig. 4E), as observed with isoprostanoids.

Previous studies demonstrated that HA accumulates in areas of WM damage and demyelination and that HA blocks OL progenitor maturation.[32,33,55] Furthermore, the HA receptor CD44 is up-regulated under conditions of free radical injury, including ischemia.[59] We therefore sought to determine the potential relevance of this mechanism in adult WM injury by immunohistochemical assessment of HA staining in relationship to Olig2+ cell density (**Figure 5**). We identified five regions of high (Fig. 5A) or low (Fig. 5B) HA immunoreactivity in each of the twenty-five PFC samples and then determined the density of Olig2+ cells in each region. HA staining was strongly associated with higher density of Olig2+ cells ($P< 0.0001$, Fig. 5C). Collectively, these data are consistent with the hypothesis that WM damage from VBI and free radical injury is characterized by reactive changes in OLs that is associated with increased accumulation of HA.

Discussion

With the advent of DTI, neuroimaging correlates of cognitive performance in elderly individuals have identified cerebral WM as a primary site of apparent injury.[6-8] The mechanisms of MRI-identified WM change have remained elusive, which has hampered progress toward the development of animal models and therapies relevant to WM change in older individuals. However, there are clues to the potential molecular mechanisms that may underlie MRI-defined WM changes in older individuals. Indeed, others also have used post mortem 1 T MRI to identify human WM lesions and observed changes of a complex pathogenesis that likely includes hypoxia- and immune-mediated damage,[60,61] and possibly an oligodendroglial precursor cell response as suggested by platelet-derived growth factor α receptor (PDGFαR) immunoreactivity, a non-specific marker of oligodendroglial precursor cells.[62] We tested this hypothesis in a population-based cohort of twenty-five consecutively collected autopsies from the ACT study where VBI and AD are prevalent and commonly co-morbid.

Novel findings from our studies were that DTI measures of PFC WM (FA and ADC) were most significantly perturbed in those samples from patients with a combination of VBI and AD, and that there was a robust relationship between decreasing FA and increasing $D_{\perp}$, consistent with WM injury suggestive of injury to myelin and axons.[54] Molecular characterization showed that increased free radical injury to fatty acids concentrated in axon membranes and myelin was significantly associated with VBI independent of AD, and with WM change, as defined by reductions in FA. Ranking of myelin damage using LFB correlated with ADC but not FA, while ranking of axonal damage as assessed by neurofilament immunohistochemistry trended with F_4-NeuroP levels. We view the latter as corroborating lines of evidence, despite not reaching statistical significance, because F_4-NeuroPs reflect a particular type of neuronal-axonal injury while morphologic evidence of axonal injury is mechanistically non-specific. Similarly, a significant expansion in the total

pool of OL cells in PFC WM was significantly associated with VBI independent of AD, and had a negative correlation with FA and a positive correlation with $D_{\perp}$, but not with $D_{\parallel}$, suggesting a relationship between WM injury and the magnitude of the reactive oligodendrocyte response. The expansion of WM OL cells coincided with elevated extracellular matrix levels of HA, an inhibitor of OL maturation in chronic WM lesions.[55]

The PFC WM samples that we analyzed derived from consecutive cases accrued through the ACT study, a population-based study of brain aging and dementia in the Seattle metropolitan area. There are well-documented differences among the prevalence of diseases that contribute to cognitive impairment and dementia in population-based *vs*. research center-based cohorts with the major difference being higher prevalence of VBI in a population-based cohort, such as ours.[63,64] Although the number of cases is not large by epidemiologic standards, they do represent a relatively unselected cohort of elderly individuals from a typical urban and suburban setting, and roughly reflect the approximate burden of diseases that injure the aging brain. In fact, we observed a prevalence and co-morbidity of AD and VBI in this group of twenty-five individuals that corresponded closely to what we have observed in the overall ACT autopsy cohort of over 250 hundred cases,[65] which in turn corresponds well with results from other population-based studies in the US and Europe.[66]

Several groups have previously used MRI to characterize postmortem CNS tissue,[46,48,49,67-73] and significant progress has been made towards understanding the degree of correspondence between *in vivo* and *ex vivo* conditions.[49,67,68,70,73] Studies in which DTI measurements were performed on the same subject prior to, and following death and tissue fixation, have shown that differences in WM FA between living and post mortem tissue are subtle, if present at all (primates[67,68]; rodents[49,73]). Specifically, Sun and co-workers recently reported that, under some conditions formalin fixation, but not death, can reduce the magnitude of the effect of ischemic injury on $D_{\parallel}$ (compensatory effects on $D_{\perp}$ preserve the overall effect on ADC and diffusion anisotropy).[74] Additionally, the water ADC decreases by a factor of ~2.5[73] after death and aldehyde fixation. This is partially due to the reduction in temperature from physiological conditions to those standard within the bore of an MRI instrument, and partially due to the destruction of various dynamic physiological processes that occur with death.[74] However, with the exception of *acute* effects of ischemia,[49] which are not relevant to this study, relative differences in ADC between neighboring brain areas are preserved.[46,73]

Comparison of biochemical and cellular changes observed in age-related WM with the pattern of MRI-identified changes suggested that DTI was less sensitive to VBI than direct determination of oxidative damage markers or the number of Olig2+ cells; the latter two modalities were sufficiently sensitive to detect changes in PFC WM with VBI alone, whereas DTI was abnormal when cases were affected by both VBI and AD. However, there was a striking correlation between quantitative *in vivo* measures of free radical injury to myelin and axonal membranes and FA across all samples. These findings suggest the possibility of a strong interaction between oxidative damage to myelin and axons and the processes that produce abnormal WM FA. Hence, isoprostanoids may be an early molecular correlate of abnormal DTI signal in adult PFC WM and thereby suggest potential preventive strategies aimed at reducing free radical injury caused by ischemia or hypoperfusion that may be intermittent, chronic, or recurrent. Identification of early biochemical markers of injury described here may guide development of more elaborate analysis of diffusion weighted images,[75-77] or additional MRI-based modalities such as susceptibility-weighted imaging[78] to provide more sensitive neuroimaging-based tools to detect oxidative damage in the future.

In the context of experimental models of ischemia[74,79] and neuroinflammatory diseases,[80] reductions in WM FA are associated with reduced $D_{\parallel}$ (interpreted as evidence of axonal injury) and increased $D_{\perp}$ (interpreted as perturbed myelin structure). The latter was observed for our cases. In contrast to the relationship between $D_{\perp}$ and FA, our $D_{\parallel}$ values differed from patterns typically found in neuroinflammatory injury. In the 23 less severely affected cases, $D_{\parallel}$ and FA were not correlated, which suggests that disruption of axonal structure defined by $D_{\parallel}$ is not a prominent feature of the cases reported here, despite evidence of free radical injury to axon membranes. However, we cannot exclude the possibility that fixation attenuates the effect of axonal injury on $D_{\parallel}$ within our sample.[74] Ultimately, histopathologic confirmation will be required, but is currently not feasible due to the lack of sensitive markers of mild to moderate axonal dysfunction where frank axonal degeneration has not occurred. In the two apparently more severe cases, $D_{\parallel}$ was *increased*, along with $D_{\perp}$, suggesting that severe injury can produce a substantially different cellular/structural environment than has been characterized in animal model studies. Although limited by the number of cases, our data suggests that for the majority of cases, increases in $D_{\perp}$ that likely result from perturbed myelin structure underlie abnormalities identified by DTI. Future studies of myelin ultra-structure are needed to define disturbances in myelination, but may not be feasible in post-mortem human tissue.

We observed pronounced expansion of OL cells in PFC WM in the setting of VBI regardless of the level of AD pathologic change, which paralleled the response for oxidative damage markers. Several potential mechanisms may account for this reactive response. The response was most closely related to $D_{\perp}$ suggesting that VBI-associated expansion of the Olig2+ population was related to WM injury, perhaps contributed to by free radical injury to myelin. This notion is consistent with the damage to myelin and the concomitant increase in OL cells observed in the WM of aged non-human primates.[81] The response may also be related to primary degeneration of oligodendrocyte precursors. In response to perinatal hypoxia-ischemia and oxidative damage, these precursors undergo both acute and delayed degeneration, which coincides with a rapid and sustained expansion of OL precursors that undergo maturation arrest in lesions with chronic gliosis.[31,55] Interestingly, the expansion of Olig2+ cells was associated with higher local levels of accumulated HA, raising the possibility of HA-dependent OL precursor maturation arrest as has been demonstrated in other settings.[29,33] One potential mechanism for the expansion of Olig2+ cells is proliferation of early OL progenitors, which are abundant in adult CNS WM.[82] In response to perinatal hypoxia-ischemia, early OL progenitors show a rapid proliferative response confirmed by increased number of Ki-67 immunoreactive nuclei. Increased Ki-67 immunoreactivity was not observed in our cases (data not shown). However, this may not be surprising given the likely chronic nature of the WM injury in older individuals. Future studies with optimally preserved human WM are needed to define what stages of OL precursors may contribute to the pronounced expansion observed in PFC WM from older adults with VBI.

As mentioned, there is considerable interest in the regional dependence of WM injury with respect to the quantity and quality of age-related cognitive impairment. While PFC WM injury is an important contributor to age-related cognitive decline, it is not the only region that is important in this complex process. However, our goal was to investigate specific cellular and molecular mechanisms or WM injury, and not to address mapping of regional WM injury to cognitive impairment. As such, our results, while directly relevant to PFC WM, may or may not be relevant to other lobes or periventricular WM. Relatedly, while antemortem MRI images would be a valuable addition to our study, it was not supported in the population-based study from which our samples were derived. However, it is important to remember that it is precisely because of this population-based study that we had the opportunity to have common examples of VBI in addition to AD.

Our observational data support the hypothesis that the mechanisms of PFC WM injury defined in our cases from older adults share similarities with some forms of WM damage sustained by preterm infants: VBI, oxidative damage, and expansion of the total OL pool with possible participation by HA (**Diagram 1**). While this form of WM injury is only one of several neuropathologic processes that may contribute to cognitive impairment in the elderly, our results do provide additional impetus to develop improved animal models of small vessel-mediated WM damage in older brains; such models will need to account for the substantial difference in the amount of WM between common laboratory animals, such as rodents, and humans. Moreover, the proposed relative timing of events in our diagram may reflect in part differing sensitivities of the techniques used, and mechanistic investigations in model systems may more clearly define the underlying biologic processes. To the extent that these models mirror the cellular and molecular characteristic of the human condition defined here, they will help provide a deeper understanding of mechanisms of WM injury in older adults and facilitate therapeutic development.

Acknowledgments

This work was supported by AG031892, AG06781, RR000163, NS045737, an Oregon Clinical Translational Institute (OCTRI) Pilot Project Grant, and the Nancy and Buster Alvord Endowment. We thank Ms. Angela Wilson and Ms. Jaime Struve for expert technical assistance, and Dr. Kathleen Montine for editorial assistance.

References

1. Ylikoski A, Erkinjuntti T, Raininko R, Sarna S, Sulkava R, Tilvis R. White matter hyperintensities on MRI in the neurologically nondiseased elderly. Analysis of cohorts of consecutive subjects aged 55 to 85 years living at home. Stroke. 1995; 26:1171–1177. [PubMed: 7604409]
2. Breteler MM, van Swieten JC, Bots ML, Grobbee DE, Claus JJ, van den Hout JH, van Harskamp F, Tanghe HL, de Jong PT, van Gijn J, et al. Cerebral white matter lesions, vascular risk factors, and cognitive function in a population-based study: the Rotterdam Study. Neurology. 1994; 44:1246–1252. [PubMed: 8035924]
3. Longstreth WT Jr. Dulberg C, Manolio TA, Lewis MR, Beauchamp NJ Jr. O'Leary D, Carr J, Furberg CD. Incidence, manifestations, and predictors of brain infarcts defined by serial cranial magnetic resonance imaging in the elderly: the Cardiovascular Health Study. Stroke. 2002; 33:2376–2382. [PubMed: 12364724]
4. Gunning-Dixon FM, Raz N. The cognitive correlates of white matter abnormalities in normal aging: a quantitative review. Neuropsychology. 2000; 14:224–232. [PubMed: 10791862]
5. DeCarli, C.; Scheltens, P. Structural brain imaging, in Vascular cognitive impairment.. In: Erkinjuntti, T.; Gauthier, S., editors. Vascular cognitive impairment. Martin Dunitz; London: 2002. p. 433-457.
6. de Groot JC, de Leeuw FE, Oudkerk M, van Gijn J, Hofman A, Jolles J, Breteler MM. Cerebral white matter lesions and cognitive function: the Rotterdam Scan Study. Ann Neurol. 2000; 47:145–151. [PubMed: 10665484]
7. de Groot JC, De Leeuw FE, Oudkerk M, Van Gijn J, Hofman A, Jolles J, Breteler MM. Periventricular cerebral white matter lesions predict rate of cognitive decline. Ann Neurol. 2002; 52:335–341. [PubMed: 12205646]
8. Brickman AM, Zimmerman ME, Paul RH, Grieve SM, Tate DF, Cohen RA, Williams LM, Clark CR, Gordon E. Regional white matter and neuropsychological functioning across the adult lifespan. Biol Psychiatry. 2006; 60:444–453. [PubMed: 16616725]
9. Salat DH, Tuch DS, Greve DN, van der Kouwe AJ, Hevelone ND, Zaleta AK, Rosen BR, Fischl B, Corkin S, Rosas HD, Dale AM. Age-related alterations in white matter microstructure measured by diffusion tensor imaging. Neurobiol Aging. 2005; 26:1215–1227. [PubMed: 15917106]
10. Kochunov P, Williamson DE, Lancaster J, Fox P, Cornell J, Blangero J, Glahn DC. Fractional anisotropy of water diffusion in cerebral white matter across the lifespan. Neurobiol Aging. 2010 epub ahead of print.

11. Murray ME, Senjem ML, Petersen RC, Hollman JH, Preboske GM, Weigand SD, Knopman DS, Ferman TJ, Dickson DW, Jack CR Jr. Functional impact of white matter hyperintensities in cognitively normal elderly subjects. Arch Neurol. 2010; 67:1379–1385. [PubMed: 21060015]
12. Marquine MJ, Attix DK, Goldstein LB, Samsa GP, Payne ME, Chelune GJ, Steffens DC. Differential patterns of cognitive decline in anterior and posterior white matter hyperintensity progression. Stroke. 2010; 41:1946–1950. [PubMed: 20651266]
13. Le Bihan D, Mangin JF, Poupon C, Clark CA, Pappata S, Molko N, Chabriat H. Diffusion tensor imaging: concepts and applications. J Magn Reson Imaging. 2001; 13:534–546. [PubMed: 11276097]
14. Neil J, Miller J, Mukherjee P, Huppi PS. Diffusion tensor imaging of normal and injured developing human brain - a technical review. NMR Biomed. 2002; 15:543–552. [PubMed: 12489100]
15. Bartzokis G, Sultzer D, Lu PH, Nuechterlein KH, Mintz J, Cummings JL. Heterogeneous age-related breakdown of white matter structural integrity: implications for cortical “disconnection” in aging and Alzheimer's disease. Neurobiol Aging. 2004; 25:843–851. [PubMed: 15212838]
16. Moseley M. Diffusion tensor imaging and aging - a review. NMR Biomed. 2002; 15:553–560. [PubMed: 12489101]
17. Pfefferbaum A, Sullivan EV, Hedehus M, Lim KO, Adalsteinsson E, Moseley M. Age-related decline in brain white matter anisotropy measured with spatially corrected echo-planar diffusion tensor imaging. Magn Reson Med. 2000; 44:259–268. [PubMed: 10918325]
18. O'Sullivan M, Jones DK, Summers PE, Morris RG, Williams SC, Markus HS. Evidence for cortical “disconnection” as a mechanism of age-related cognitive decline. Neurology. 2001; 57:632–638. [PubMed: 11524471]
19. Head D, Buckner RL, Shimony JS, Williams LE, Akbudak E, Conturo TE, McAvoy M, Morris JC, Snyder AZ. Differential vulnerability of anterior white matter in nondemented aging with minimal acceleration in dementia of the Alzheimer type: evidence from diffusion tensor imaging. Cereb Cortex. 2004; 14:410–423. [PubMed: 15028645]
20. Madden DJ, Whiting WL, Huettel SA, White LE, MacFall JR, Provenzale JM. Diffusion tensor imaging of adult age differences in cerebral white matter: relation to response time. Neuroimage. 2004; 21:1174–1181. [PubMed: 15006684]
21. Shenkin SD, Bastin ME, Macgillivray TJ, Deary IJ, Starr JM, Rivers CS, Wardlaw JM. Cognitive correlates of cerebral white matter lesions and water diffusion tensor parameters in community-dwelling older people. Cerebrovasc Dis. 2005; 20:310–318. [PubMed: 16141715]
22. Reed BR, Mungas DM, Kramer JH, Ellis W, Vinters HV, Zarow C, Jagust WJ, Chui HC. Profiles of neuropsychological impairment in autopsy-defined Alzheimer's disease and cerebrovascular disease. Brain. 2007; 130:731–739. [PubMed: 17267522]
23. Buckner RL. Memory and executive function in aging and AD: multiple factors that cause decline and reserve factors that compensate. Neuron. 2004; 44:195–208. [PubMed: 15450170]
24. Iadecola C, Hachinski V, Rosenberg GA. Vascular cognitive impairment: introduction. Stroke. 2010; 41:S127–128. [PubMed: 20876487]
25. Hachinski V. The 2005 Thomas Willis Lecture: stroke and vascular cognitive impairment: a transdisciplinary, translational and transactional approach. Stroke. 2007; 38:1396. [PubMed: 17347469]
26. Brown WR, Thore CR. Review: cerebral microvascular pathology in ageing and neurodegeneration. Neuropathol Appl Neurobiol. 2011; 37:56–74. [PubMed: 20946471]
27. Fernando MS, O'Brien JT, Perry RH, English P, Forster G, McMeekin W, Slade JY, Golkhar A, Matthews FE, Barber R, Kalaria RN, Ince PG. Comparison of the pathology of cerebral white matter with post-mortem magnetic resonance imaging (MRI) in the elderly brain. Neuropathol Appl Neurobiol. 2004; 30:385–395. [PubMed: 15305984]
28. Haynes RL, Folkerth RD, Keefe RJ, Sung I, Swzeda LI, Rosenberg PA, Volpe JJ, Kinney HC. Nitrosative and oxidative injury to premyelinating oligodendrocytes in periventricular leukomalacia. J Neuropathol Exp Neurol. 2003; 62:441–450. [PubMed: 12769184]
29. Back SA, Tuohy TM, Chen H, Wallingford N, Craig A, Struve J, Luo NL, Banine F, Liu Y, Chang A, Trapp BD, Bebo BF Jr. Rao MS, Sherman LS. Hyaluronan accumulates in demyelinated

lesions and inhibits oligodendrocyte progenitor maturation. Nat Med. 2005; 11:966–972. [PubMed: 16086023]

30. Back SA, Han BH, Luo NL, Chricton CA, Xanthoudakis S, Tam J, Arvin KL, Holtzman DM. Selective vulnerability of late oligodendrocyte progenitors to hypoxia-ischemia. J Neurosci. 2002; 22:455–463. [PubMed: 11784790]
31. Segovia KN, McClure M, Moravec M, Luo NL, Wan Y, Gong X, Riddle A, Craig A, Struve J, Sherman LS, Back SA. Arrested oligodendrocyte lineage maturation in chronic perinatal white matter injury. Ann Neurol. 2008; 63:520–530. [PubMed: 18393269]
32. Struve J, Maher PC, Li YQ, Kinney S, Fehlings MG, Kuntz Ct, Sherman LS. Disruption of the hyaluronan-based extracellular matrix in spinal cord promotes astrocyte proliferation. Glia. 2005; 52:16–24. [PubMed: 15892130]
33. Sloane JA, Batt C, Ma Y, Harris ZM, Trapp B, Vartanian T. Hyaluronan blocks oligodendrocyte progenitor maturation and remyelination through TLR2. Proc Natl Acad Sci U S A. 2010; 107:11555–11560. [PubMed: 20534434]
34. Buffo A, Vosko MR, Erturk D, Hamann GF, Jucker M, Rowitch D, Gotz M. Expression pattern of the transcription factor Olig2 in response to brain injuries: implications for neuronal repair. Proc Natl Acad Sci U S A. 2005; 102:18183–18188. [PubMed: 16330768]
35. Larson EB, Wang L, Bowen JD, McCormick WC, Teri L, Crane P, Kukull W. Exercise is associated with reduced risk for incident dementia among persons 65 years of age and older. Ann Intern Med. 2006; 144:73–81. [PubMed: 16418406]
36. Wang L, Larson EB, Bowen JD, van Belle G. Performance-based physical function and future dementia in older people. Arch Intern Med. 2006; 166:1115–1120. [PubMed: 16717174]
37. Sonnen JA, Larson EB, Gray SL, Wilson A, Kohama SG, Crane PK, Breitner JC, Montine TJ. Free radical damage to cerebral cortex in Alzheimer's disease, microvascular brain injury, and smoking. Ann Neurol. 2009; 65:226–229. [PubMed: 19259965]
38. Sonnen JA, Larson EB, Crane PK, Haneuse S, Li G, Schellenberg GD, Craft S, Leverenz JB, Montine TJ. Pathological correlates of dementia in a longitudinal, population-based sample of aging. Ann Neurol. 2007; 62:406–413. [PubMed: 17879383]
39. Consensus recommendations for the postmortem diagnosis of Alzheimer's disease. The National Institute on Aging, and Reagan Institute Working Group on Diagnostic Criteria for the Neuropathological Assessment of Alzheimer's Disease. Neurobiol Aging. 1997; 18:S1–2. [PubMed: 9330978]
40. White L, Petrovitch H, Hardman J, Nelson J, Davis DG, Ross GW, Masaki K, Launer L, Markesbery WR. Cerebrovascular pathology and dementia in autopsied Honolulu-Asia Aging Study participants. Ann N Y Acad Sci. 2002; 977:9–23. [PubMed: 12480729]
41. Leverenz JB, Hamilton R, Tsuang DW, Schantz A, Vavrek D, Larson EB, Kukull WA, Lopez O, Galasko D, Masliah E, Kaye J, Woltjer R, Clark C, Trojanowski JQ, Montine TJ. Empiric refinement of the pathologic assessment of Lewy-related pathology in the dementia patient. Brain Pathol. 2008; 18:220–224. [PubMed: 18241240]
42. VanRollins M, Woltjer RL, Yin H, Morrow JD, Montine TJ. F2-dihomoisoprostanes arise from free radical attack on adrenic acid. J Lipid Res. 2008; 49:995–1005. [PubMed: 18250368]
43. Kadiiska MB, Gladen BC, Baird DD, Germolec D, Graham LB, Parker CE, Nyska A, Wachsman JT, Ames BN, Basu S, Brot N, Fitzgerald GA, Floyd RA, George M, Heinecke JW, Hatch GE, Hensley K, Lawson JA, Marnett LJ, Morrow JD, Murray DM, Plastaras J, Roberts LJ 2nd, Rokach J, Shigenaga MK, Sohal RS, Sun J, Tice RR, Van Thiel DH, Wellner D, Walter PB, Tomer KB, Mason RP, Barrett JC. Biomarkers of oxidative stress study II: are oxidation products of lipids, proteins, and DNA markers of CCl4 poisoning? Free Radic Biol Med. 2005; 38:698–710. [PubMed: 15721980]
44. Kadiiska MB, Gladen BC, Baird DD, Graham LB, Parker CE, Ames BN, Basu S, Fitzgerald GA, Lawson JA, Marnett LJ, Morrow JD, Murray DM, Plastaras J, Roberts LJ 2nd, Rokach J, Shigenaga MK, Sun J, Walter PB, Tomer KB, Barrett JC, Mason RP. Biomarkers of oxidative stress study III. Effects of the nonsteroidal anti-inflammatory agents indomethacin and meclofenamic acid on measurements of oxidative products of lipids in CCl4 poisoning. Free Radic Biol Med. 2005; 38:711–718. [PubMed: 15721981]

45. Roberts LJ 2nd, Montine TJ, Markesbery WR, Tapper AR, Hardy P, Chemtob S, Dettbarn WD, Morrow JD. Formation of isoprostane-like compounds (neuroprostanes) in vivo from docosahexaenoic acid. J Biol Chem. 1998; 273:13605–13612. [PubMed: 9593698]
46. Kroenke CD, Bretthorst GL, Inder TE, Neil JJ. Diffusion MR imaging characteristics of the developing primate brain. Neuroimage. 2005; 25:1205–1213. [PubMed: 15850738]
47. Kroenke CD, Bretthorst GL, Inder TE, Neil JJ. Modeling water diffusion anisotropy within fixed newborn primate brain using Bayesian probability theory. Magn Reson Med. 2006; 55:187–197. [PubMed: 16342153]
48. Kroenke CD, Van Essen DC, Inder TE, Rees S, Bretthorst GL, Neil JJ. Microstructural changes of the baboon cerebral cortex during gestational development reflected in magnetic resonance imaging diffusion anisotropy. J. Neurosci. 2007; 27:12506–12515. [PubMed: 18003829]
49. Sun SW, Neil JJ, Liang HF, He YY, Schmidt RE, Hsu CY, Song SK. Formalin fixation alters water diffusion coefficient magnitude but not anisotropy in infarcted brain. Magn Reson Med. 2005; 53:1447–1451. [PubMed: 15906292]
50. Batchelor PG, Atkinson D, Hill DL, Calamante F, Connelly A. Anisotropic noise propagation in diffusion tensor MRI sampling schemes. Magn Reson Med. 2003; 49:1143–1151. [PubMed: 12768593]
51. Basser PJ, Pierpaoli C. Microstructural and physiological features of tissues elucidated by quantitative-diffusion-tensor MRI. J Magn Reson B. 1996; 111:209–219. [PubMed: 8661285]
52. Yushkevich PA, Piven J, Hazlett HC, Smith RG, Ho S, Gee JC, Gerig G. User-guided 3D active contour segmentation of anatomical structures: significantly improved efficiency and reliability. Neuroimage. 2006; 31:1116–1128. [PubMed: 16545965]
53. Montine TJ, Sonnen JA, Montine KS, Crane PK, Larson EB. Adult Changes in Thought Study: Dementia is an individually varying convergent syndrome with prevalent clinically silent diseases that may be modified by some commonly used therapeutics. Current Alzheimer Research. in press.
54. Song SK, Sun SW, Ramsbottom MJ, Chang C, Russell J, Cross AH. Dysmyelination revealed through MRI as increased radial (but unchanged axial) diffusion of water. Neuroimage. 2002; 17:1429–1436. [PubMed: 12414282]
55. Back SA, Luo NL, Mallinson RA, O'Malley JP, Wallen LD, Frei B, Morrow JD, Petito CK, Roberts CT Jr. Murdoch GH, Montine TJ. Selective vulnerability of preterm white matter to oxidative damage defined by F2-isoprostanes. Ann Neurol. 2005; 58:108–120. [PubMed: 15984031]
56. Rivers LE, Young KM, Rizzi M, Jamen F, Psachoulia K, Wade A, Kessaris N, Richardson WD. PDGFRA/NG2 glia generate myelinating oligodendrocytes and piriform projection neurons in adult mice. Nat Neurosci. 2008; 11:1392–1401. [PubMed: 18849983]
57. Islam MS, Tatsumi K, Okuda H, Shiosaka S, Wanaka A. Olig2-expressing progenitor cells preferentially differentiate into oligodendrocytes in cuprizone-induced demyelinated lesions. Neurochem Int. 2009; 54:192–198. [PubMed: 19070638]
58. Geha S, Pallud J, Junier MP, Devaux B, Leonard N, Chassoux F, Chneiweiss H, Daumas-Duport C, Varlet P. NG2+/Olig2+ cells are the major cycle-related cell population of the adult human normal brain. Brain Pathol. 2010; 20:399–411. [PubMed: 19486010]
59. Wang H, Zhan Y, Xu L, Feuerstein GZ, Wang X. Use of suppression subtractive hybridization for differential gene expression in stroke: discovery of CD44 gene expression and localization in permanent focal stroke in rats. Stroke. 2001; 32:1020–1027. [PubMed: 11283406]
60. Simpson JE, Hosny O, Wharton SB, Heath PR, Holden H, Fernando MS, Matthews F, Forster G, O'Brien JT, Barber R, Kalaria RN, Brayne C, Shaw PJ, Lewis CE, Ince PG. Microarray RNA expression analysis of cerebral white matter lesions reveals changes in multiple functional pathways. Stroke. 2009; 40:369–375. [PubMed: 19109541]
61. Fernando MS, Simpson JE, Matthews F, Brayne C, Lewis CE, Barber R, Kalaria RN, Forster G, Esteves F, Wharton SB, Shaw PJ, O'Brien JT, Ince PG. White matter lesions in an unselected cohort of the elderly: molecular pathology suggests origin from chronic hypoperfusion injury. Stroke. 2006; 37:1391–1398. [PubMed: 16627790]
62. Simpson JE, Fernando MS, Clark L, Ince PG, Matthews F, Forster G, O'Brien JT, Barber R, Kalaria RN, Brayne C, Shaw PJ, Lewis CE, Wharton SB. White matter lesions in an unselected

cohort of the elderly: astrocytic, microglial and oligodendrocyte precursor cell responses. Neuropathol Appl Neurobiol. 2007; 33:410–419. [PubMed: 17442062]

63. Schneider JA, Aggarwal NT, Barnes L, Boyle P, Bennett DA. The neuropathology of older persons with and without dementia from community versus clinic cohorts. J Alzheimers Dis. 2009; 18:691–701. [PubMed: 19749406]
64. Massoud F, Devi G, Stern Y, Lawton A, Goldman JE, Liu Y, Chin SS, Mayeux R. A clinicopathological comparison of community-based and clinic-based cohorts of patients with dementia. Arch Neurol. 1999; 56:1368–1373. [PubMed: 10555657]
65. Sonnen JA, Larson EB, Walker RL, Haneuse S, Crane PK, Gray SL, Breitner JC, Montine TJ. Nonsteroidal anti-inflammatory drugs are associated with increased neuritic plaques. Neurology. 2010; 75:1203–1210. [PubMed: 20811000]
66. Schneider JA, Bennett DA. Where vascular meets neurodegenerative disease. Stroke. 2010; 41:S144–146. [PubMed: 20876491]
67. D'Arceuil H, de Crespigny A. The effects of brain tissue decomposition on diffusion tensor imaging and tractography. Neuroimage. 2007; 36:64–68. [PubMed: 17433879]
68. D'Arceuil HE, Westmoreland S, de Crespigny AJ. An approach to high resolution diffusion tensor imaging in fixed primate brain. Neuroimage. 2007; 35:553–565. [PubMed: 17292630]
69. Flynn SW, Lang DJ, Mackay AL, Goghari V, Vavasour IM, Whittall KP, Smith GN, Arango V, Mann JJ, Dwork AJ, Falkai P, Honer WG. Abnormalities of myelination in schizophrenia detected in vivo with MRI, and post-mortem with analysis of oligodendrocyte proteins. Molecular psychiatry. 2003; 8:811–820. [PubMed: 12931208]
70. Guilfoyle DN, Helpern JA, Lim KO. Diffusion tensor imaging in fixed brain tissue at 7.0 T. NMR Biomed. 2003; 16:77–81. [PubMed: 12730948]
71. Mori S, Itoh R, Zhang J, Kaufmann WE, van Zijl PC, Solaiyappan M, Yarowsky P. Diffusion tensor imaging of the developing mouse brain. Magn Reson Med. 2001; 46:18–23. [PubMed: 11443706]
72. Pfefferbaum A, Sullivan EV, Adalsteinsson E, Garrick T, Harper C. Postmortem MR imaging of formalin-fixed human brain. Neuroimage. 2004; 21:1585–1595. [PubMed: 15050582]
73. Sun SW, Neil JJ, Song SK. Relative indices of water diffusion anisotropy are equivalent in live and formalin-fixed mouse brains. Magn Reson Med. 2003; 50:743–748. [PubMed: 14523960]
74. Sun SW, Liang HF, Xie M, Oyoyo U, Lee A. Fixation, not death, reduces sensitivity of DTI in detecting optic nerve damage. Neuroimage. 2009; 44:611–619. [PubMed: 19027864]
75. Ozarslan E, Mareci TH. Generalized diffusion tensor imaging and analytical relationships between diffusion tensor imaging and high angular resolution diffusion imaging. Magn Reson Med. 2003; 50:955–965. [PubMed: 14587006]
76. Assaf Y, Basser PJ. Composite hindered and restricted model of diffusion (CHARMED) MR imaging of the human brain. Neuroimage. 2005; 27:48–58. [PubMed: 15979342]
77. Jensen JH, Helpern JA, Ramani A, Lu H, Kaczynski K. Diffusional kurtosis imaging: the quantification of non-gaussian water diffusion by means of magnetic resonance imaging. Magn Reson Med. 2005; 53:1432–1440. [PubMed: 15906300]
78. Haacke EM, Mittal S, Wu Z, Neelavalli J, Cheng YC. Susceptibility-weighted imaging: technical aspects and clinical applications, part 1. AJNR Am J Neuroradiol. 2009; 30:19–30. [PubMed: 19039041]
79. Song SK, Sun SW, Ju WK, Lin SJ, Cross AH, Neufeld AH. Diffusion tensor imaging detects and differentiates axon and myelin degeneration in mouse optic nerve after retinal ischemia. Neuroimage. 2003; 20:1714–1722. [PubMed: 14642481]
80. Budde MD, Xie M, Cross AH, Song SK. Axial diffusivity is the primary correlate of axonal injury in the experimental autoimmune encephalomyelitis spinal cord: a quantitative pixelwise analysis. J Neurosci. 2009; 29:2805–2813. [PubMed: 19261876]
81. Peters A. The effects of normal aging on myelinated nerve fibers in monkey central nervous system. Front Neuroanat. 2009; 3:11. [PubMed: 19636385]
82. Nishiyama A, Komitova M, Suzuki R, Zhu X. Polydendrocytes (NG2 cells): multifunctional cells with lineage plasticity. Nat Rev Neurosci. 2009; 10:9–22. [PubMed: 19096367]

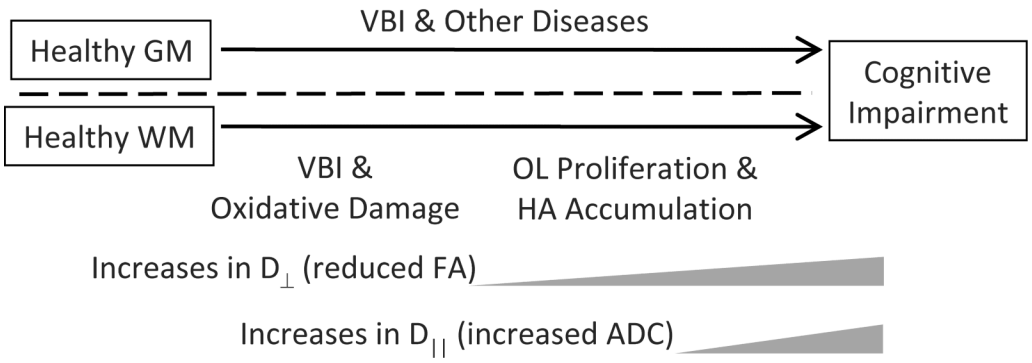

Diagram 1.

Diagram that shows a proposed relationship among biochemical, cellular, and imaging endpoints of white matter (WM) injury and it consequences on cognitive function in the context of other common co-morbid diseases that target primarily gray matter (GM). Abbreviations: Vascular Brain Injury (VBI), oligodendrocyte lineage (OL), hyaluronan (HA), fractional anisotropy (FA), apparent diffusion coefficient (ADC), radial diffusivity ($D_{\perp}$), and axial diffusivity ($D_{\parallel}$).

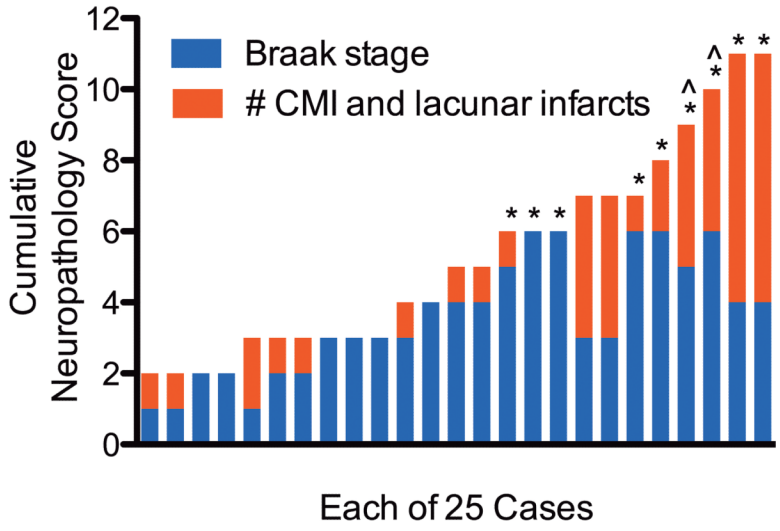

Figure 1.

The burden of Alzheimer's disease (AD) and vascular brain injury (VBI) is represented for each of the twenty-five individuals that met criteria for our study by Braak stage for neurofibrillary tangles (range 0 to 6) and the sum of the number of cerebral microinfarcts plus the number of lacunar infarcts. No individual in this group had cerebral cortical Lewy body disease. *Individuals diagnosed with dementia by DSM-IVR criteria within two years of death. ^Cases with especially low fractional anisotropy.

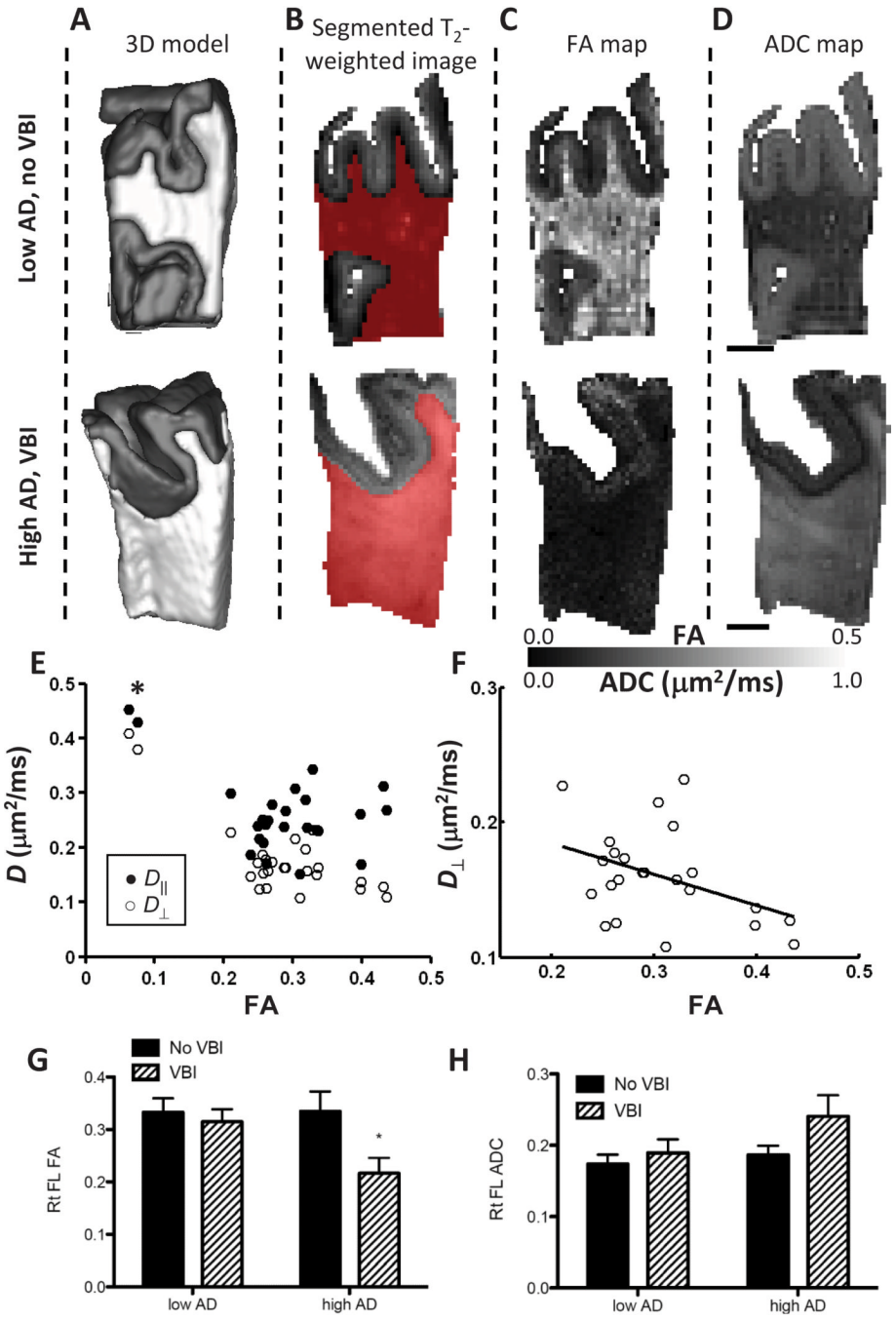

Figure 2. Diffusion-based MRI contrast of right PFC WM from humans

Fixed tissue samples were imaged in a standard orientation **(A)** presented as 3-D model or (**B**) T_2-weighted images that classify image voxels (volumetric pixels) as GM or WM. **(C-D)** Individual slices from 3-D of fractional anisotropy (FA) and apparent diffusion coefficient (ADC) parameter maps from Low AD/No VBI case and High AD/VBI case are shown. We observed increased ADC and decreased FA in WM from this most severely damaged case from the High AD/VBI group. **(E)** Scatter plot of $D_{\parallel}$ vs. $D_{\perp}$ or all twenty-five cases regardless of pathologic classification with (**F**) best-fit line calculated while excluding the two cases with extremely low FA. **(G-H)** Mean ± SEM FA and ADC values for the four pathologic groups. Two way ANOVA showed that FA (G) significantly varied with

presence or absence of VBI ($P < 0.05$) but not with ADC (H); there was no significant interaction between VBI and AD for FA or ADC. Multiple comparison-corrected post tests showed that relationship to FA resided with the High AD/VBI group (*$P < 0.05$).

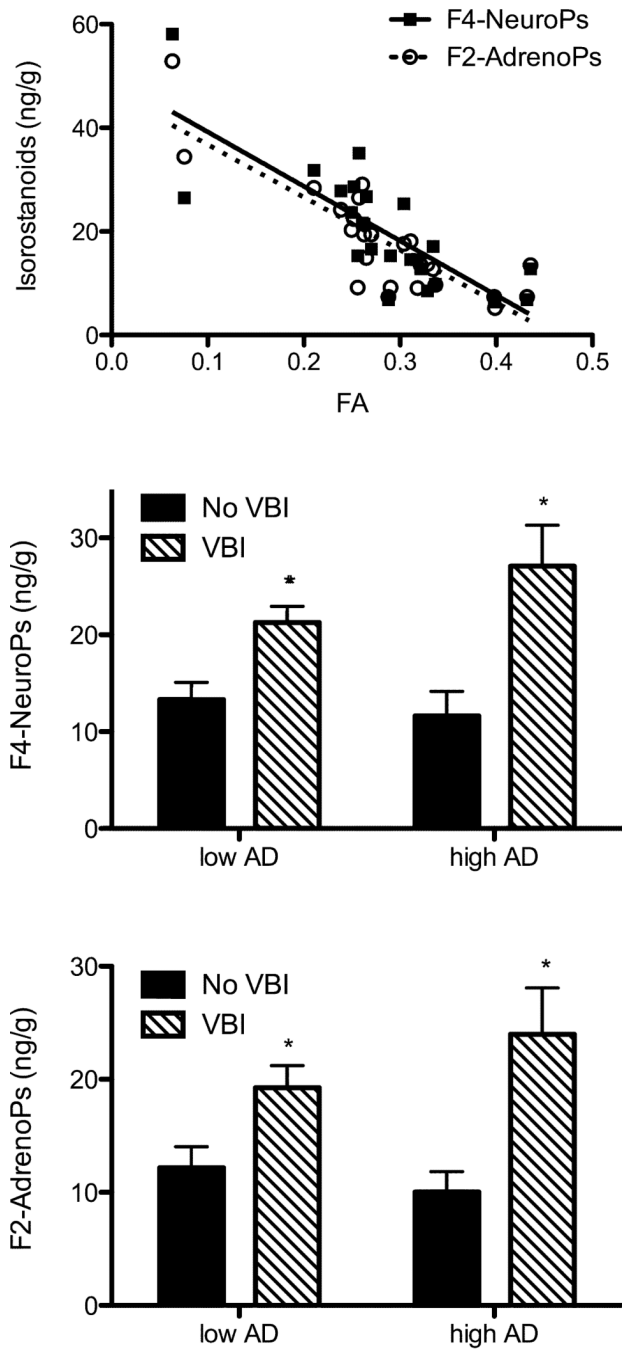

Figure 3.

Indices of free radical injury in human right pre-frontal cortical (PFC) white matter (WM). Samples immediately adjacent to those used to MRI measures were flash frozen in liquid nitrogen and stored at -80°C until extracted and analyzed with stable isotope dilution assay using gas chromatography/mass spectrometry and selective ion monitoring for the isoprostanoids F_4-Neuroprostanes (NeuroPs) and F_2-Adrenoprostanes (AdrenoPs). (**A**). Scatter plot with best-fit line for isoprostanoids (ng/g) vs. FA for all twenty-five PFC WM samples: F_4-NeuroP ($r = -0.80$, $P < 0.0001$), and F_2-AdrenoP ($r = -0.84$, $P < 0.0001$). (**B and C**). Stratification of isoprostanoid data (ng/g) by four pathologically determined disease groups. Two-way ANOVA for F_4-NeuroPs (B) had $P < 0.01$ for VBI and for F_2-AdrenoPs

(C) had $P < 0.05$ for VBI; both isoprostanoids had $P > 0.05$ for AD or interaction. Multiple comparison-corrected post tests had $^{*}P < 0.05$ for both F_4-NeuroPs and F_2-AdrenoPs in groups with VBI regardless of Low or High AD.

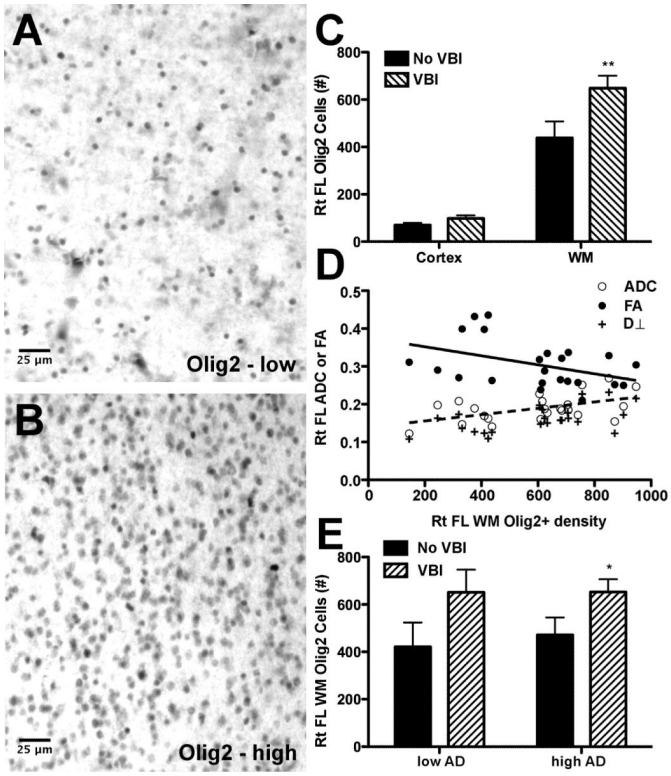

Figure 4.

Density of cells with Olig2-immunoreactive nuclei (Olig2+) in pre-frontal cortical (PFC) samples. (**A and B**) Within white matter (WM), the number of Olig2+ cells varied from cases with low density (**A**) to cases with an apparent reactive response that had high Olig2 + cell density (**B**). (**C**) Olig2+ cell density in WM and overlying gray matter (GM) from the twenty-five PFC tissue blocks that underwent MRI; two-way ANOVA $P < 0.001$ for cortical GM vs. WM, $P < 0.01$ for presence or absence of vascular brain injury (VBI), and $P < 0.05$ for interaction between these terms. Multiple comparison-corrected post tests had $^{**}P < 0.01$ for WM no VBI vs. WM with VBI. (**D**) Scatter plot of DTI measures vs. Olig2+ cell density in twenty-three PFC WM samples with less extreme injury and corresponding best-fit line for FA (solid line, $P < 0.05$) and ADC (dashed line, $P < 0.05$). The linear relationship between Olig2+ cell density was strongest with $D_{\perp}$ ($P < 0.01$). (**E**) Stratification of Olig2+ cell density into the four pathologic groups. Two-way ANOVA had $P < 0.05$ for VBI but not AD. Multiple comparison-corrected post tests had $^{*}P < 0.05$ for VBI vs. no VBI in both the Low and High AD groups.

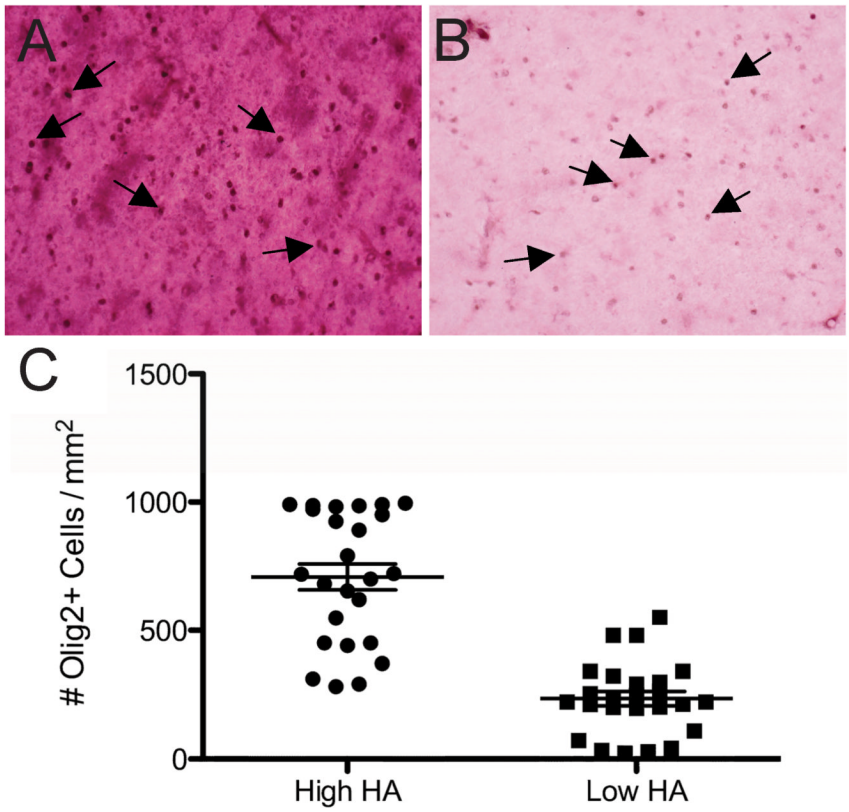

Figure 5.

Photomicrographs of double immunohistochemistry in PFC WM. **(A)**: Representative high HA area with intense HABP staining. **(B):** Representative low HA area with weak HABP staining. Cells with Olig2+ nuclei (arrows) are shown in both areas. (**C**) Paired t test for Olig2+ cell density in high vs. low HA areas for the twenty-five PFC WM samples ($P < 0.0001$).

Table 1

“Low AD” (Alzheimer's disease) is defined as Braak stage for neurofibrillary tangles (NFTs) I, II, or III (no one had no NFTs) and “High AD” as Braak stages IV, VI, or VI. “No VBI” (vascular brain injury) is defined as no gross (territorial or lacunar infarcts) infarcts or cerebral microinfarcts (CMIs) while VBI is defined as any CMI; all gross infarcts occurred in cases with CMI.

		Low AD	High AD
No VBI	N	5	3
	Age (yr)	85 ± 7	88 ± 3
	F : M	3 : 2	2 : 1
	PMI (hr)	4 ± 2	4 ± 1
	Brain wt (g)	1298 ± 111	1053 ± 48
VBI	N	8	9
	Age (yr)	85 ± 6	87 ± 6
	F : M	3 : 5	5 : 4
	PMI (hr)	4 ± 1	5 ± 2
	Brain wt (g)	1205 ± 117	1127 ± 109

Abbreviation: post mortem interval (PMI).